Analysis of the Impact of EMF Restrictions on 5G Base Stations Deployment in Existing Networks

Frederico Maia e Moura, Luís M. Correia
Instituto Superior Técnico / INOV-INESC
University of Lisbon
Lisbon, Portugal
frederico.maia.moura@tecnico.ulisboa.pt
luis.m.correia@tecnico.ulisboa.pt

Luís Taborda
Huawei
Lisbon, Portugal
luis.taborda@huawei.com

***Abstract* —This thesis aims at developing a model to analyse the impact of electromagnetic field restrictions on NR performance in base stations (BSs) with co-location of GSM, UMTS and LTE. A model to estimate the exclusion region of BS antennas was developed. The model estimates the power density as a function of distance for each mobile communication system and any given direction, using far- and near-fields models. One considers that the antennas are continuously radiating at maximum power as a worst-case perspective. A model for the computation of the coverage radius and throughput per resource block (RB) as a function of the NR BS transmitted power was developed. Representative scenarios of BSs with co-location of antennas are analysed. An analysis of the exclusion zone distance is made before and after the installation of NR; for urban scenarios, the highest increase is 248.7%, while it is 131.6% and 56.4% for the suburban and rural ones, respectively. The impact of exclusion zones with restricted dimensions on the coverage radius and throughput per RB at cell-edge is analysed. The highest decrease in coverage radius is 62.9% for rural scenarios and 63.3% for suburban ones; regarding throughput, the highest decrease is 95.9% for both urban and suburban environments. Results show that, in some scenarios, operators may need to reduce the power transmitted by NR and legacy systems in order to comply with exclusion zone restrictions.**

Keywords - Exclusion Zones, Mobile Communications Systems, Antennas, Coverage, Throughput, NR.

I. INTRODUCTION

According to [1], the total number of mobile subscriptions reached 8.3 billion in 2019. With a global population of around 7.7 billion in 2020, the number of devices connected to cellular networks has already exceeded the number of people on the planet. As connectivity becomes more and more vital to the general public, as well as to companies and commerce in general, the number of connected devices increases, and thus traffic and capacity demands for the cellular networks also increase. The fifth-generation (5G), also known as New Radio (NR), offers the solution to this problem by implementing a network with a higher device capacity, higher offered throughput and also extremely low latency. High gain antennas and other new techniques, such as beamforming and massive MIMO (MaMIMO), help increasing the system coverage and capacity.

Since the beginning of mobile communications systems, awareness has been raised and studies have been performed on the potential health risk caused by electromagnetic radiation from these systems. Due to the increase in BS deployment, the popularity of these systems and massive publicly available information, the general public has been more and more concerned about the research and impact of Electromagnetic Fields (EMFs) on the human body. The International Commission on Non-Ionising Radiation Protection (ICNIRP) is a scientific body that works together with experts from different countries and fields, such as biology, epidemiology, medicine, physics and chemistry to assess the risk of non-ionising radiation (NIR) exposure, and provide guidelines for the maximum allowed exposure levels from the quantification of adverse health effects. Most European countries, such as Portugal, adopt these reference threshold values established by the ICNIRP, although there are countries that establish their own exposure guidelines with lower values than the ones established by ICNIRP. Mobile communications operators are obliged to comply with the limits imposed by their respective countries.

In the vicinity of BS antennas, exposure levels may be higher than the ones defined in the guidelines. Such regions are called the exclusion zone of a BS and, if they are in regions accessible to the general public, physical barriers should be implemented by operators in order to protect the public from potentially dangerous levels of radiation. A sketch of an exclusion zone represented by an imaginary semi-sphere and limited by physical barriers is illustrated in Figure 1. EMF measurement campaigns, electromagnetic (EM) simulations and mathematical models can be performed to assess EMF compliance near BS antennas.

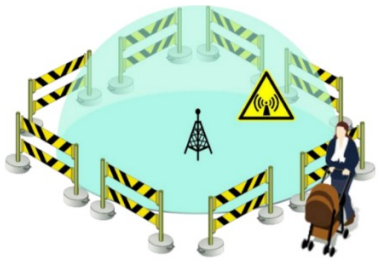

Figure 1. BS exclusion zone delimited by physical barriers (extracted from [2]).

With each new mobile communications system generation, and since in Portugal no system has been decommissioned, the number of active systems increases. In order to reduce the costs of network deployment, operators take advantage of legacy BSs to install NR antennas. Since these BSs already possess GSM, UMTS and LTE, the addition of another system increases the exposure levels near the BS, thus increasing the size of the exclusion zone around it. In BS installations where the exclusion zone must have limited dimensions, a decrease in the transmitted power may be necessary, thus affecting network roll-out and performance.

The purpose of this work was to develop a model, and a simulator to implement it, to compute the exclusion zone of a BS in order to understand the impact of NR installations on the increase of the existing exclusion regions, and to verify in which

circumstances this increase requires the definition of physical barriers for public protection. The evaluation of the exposure levels in the vicinity of the BSs requires the knowledge of several antenna parameters, such as transmitted power, radiation patterns, and frequency band. The implemented model is also used to analyse the impact of EMF restrictions implemented at the BSs on coverage and throughput. In the BSs where already exists some degree of EMF saturation prior to the installation of NR, restrictions must be implemented at the level of the transmission powers of NR antennas. These restrictions have a negative impact on the quality of the services offered by operators and create difficulties in the process of NR network roll-out.

This paper is presented as follows: Section I – Introduction; Section II – Fundamental Aspects and State of the Art; Section III – Model Development and Simulator; Section IV – Results Analysis; Section V – Conclusions.

II. Fundamental Aspects and State of the Art

A. Fundamental Aspects

From a health risk perspective, there is the need to know how much EMF power is absorbed by biological tissue, as this is responsible for the possible adverse thermal effects. This EMF power absorbing capability is typically a function of the incident field frequency. As stated in [3], for frequencies below 6 GHz it is useful to describe this effect in terms of the Specific Absorption Rate (SAR), which is the power absorbed per unit mass (W kg^{-1}), since for these frequencies EMFs penetrate deep into tissue and thus depth needs to be considered. Since SAR can be difficult to measure, other, more easily evaluated quantities, named reference levels, are also specified. These quantities relevant to the guidelines are the Electric field (E), the Magnetic field (H), and the Power Density (S).

The reference levels for the general public regarding E, H, and S, for exposures higher than 6 minutes that are under the frequencies of interest in this work are represented in Table 1 and Figure 2.

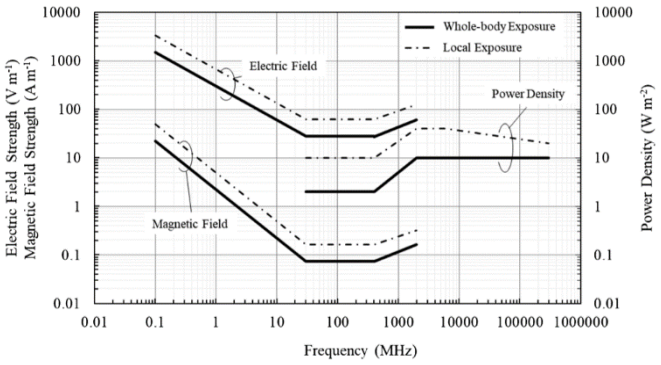

Figure 2. Reference levels for time-averaged exposures of ≥ 6 minutes from 100 kHz to 300 GHz (extracted from [2]).

Table 1. Reference levels for whole body exposure to EMF fields (adapted from [2]).

Frequency Range, f [MHz]	E (V×m^{-1})	H (A×m^{-1})	S (W×m^{-2})
]400, 2000]	1.375×f$^{0.5}$	0.0037×f$^{0.5}$	f/200
> 2000	----	----	10

It is important to observe that in situations of simultaneous exposure to fields of different frequencies, these exposures are additive in their effect, and thus it is possible to analyse separately each frequency exposure. The following criterion regarding the reference values for the power density should then be applied as:

$$\sum_{i=30\ \mathrm{MHz}}^{300\ \mathrm{GHz}} \left(\frac{S_{i,[\mathrm{W/m^2}]}}{S_{ref,i,[\mathrm{W/m^2}]}} \right) \leq 1 \qquad (2.1)$$

where:

- S_i: the power density at frequency i;
- $S_{ref,i}$: the power density reference level from Table 1 at frequency i.

Measurement procedures to assess EMF components, as well as the maximum localised SAR in a human model, can be time-consuming and BS type dependent [4]. As an alternative to these procedures, software simulations of EMFs around BS antennas may be run, although this approach typically requires a large amount of time to obtain precise results. The most practical solution to assess EMF levels, and int turn estimate exclusion zones around BSs, is to select adequate mathematical models, which usually provide a good prediction of radiation levels and are simple to apply. In [5], several models for the estimation of EMFs around BS antennas are presented:

- Far-field model;
- Far-field approximation;
- Cylindrical exclusion zone;
- Far-field gain-based model;
- Synthetic and gain-based model;
- Hybrid prediction.

A model for the representation of an exclusion zone of a BS antenna is illustrated in Figure 3.

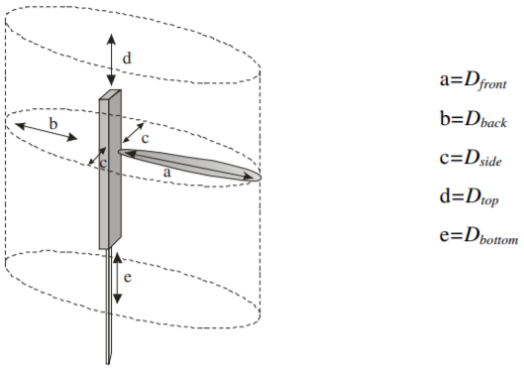

Figure 3. Representation of an antenna's exclusion zone (extracted from [5]).

The distance values calculated from these models are obtained for the worst-case scenario and in the direction of the antenna's main lobe (D_{front}). In order to obtain the distances for the sides (D_{side}), back (D_{back}), top (D_{top}) and bottom of the antenna (D_{bottom}), correction factors are applied to D_{front}, which depends on the desired direction. These correction factors are determined from the typical antenna characteristics found in the antenna's catalogue.

The values for the exclusion zone distances, as well as the need to implement physical barriers for public protection, depend on the type of BS antennas installation. Regarding BS installation type, different types of BSs require different proximities to the general public, which, depending on the transmitted powers, may require the need for physical barriers. The classification of different types of infrastructure supporting the BS antennas for the interest of this work, as well as the respective cell type and the involving environment, are presented in Table 2.

Table 2. Classification of BS antennas installation (extracted from [5] and [2]).

Denomination	Cell Type	Environment	Installation Type	Antenna Height [m]
Rtower	Macrocell	Rural, Suburban	Tower, Mast, Water sump, "Tree"	20-50
Uroof	Micro/Macrocell*	Urban	Roof-top	2-5**
Utower			Tower	20-40
Ufaçade	Microcell		Bulding Façade	3-10
Upole			Light Pole or other	3-5

*: The cell type will depend on the coverage area
**: Height from the rooftop

B. State of the Art

In this thesis, the problem addressed is the installation of NR BSs in sites with legacy technologies, also termed the Brownfield approach. In [6] two real-world case-studies of currently deployed cellular networks are considered to support the discussion of the impact of EMF restrictions on NR network planning.

The first case-study concentrates on a portion of the Fuorigrotta district, in Naples, Italy, and the main goal is to assess the EMF levels in the given area. The results show that for the maximum input power and 75% of the maximum input power, there are several zones within the studied area that exceeds the Italian limits for EMF exposure. These results highlight the concern that some areas may already have reached EMF saturation with the use of legacy networks, which can significantly limit the deployment of future NR BSs. It is important to note that the limits imposed by the Italian government are considerably below the ones proposed by ICNIRP.

The second case study focuses on the impact of current regulations on network planning and the QoS offered to the end-user on the Torrino Mezzocammino (TMC) area in Rome, Italy. To this end, [6] used CellMapper, a monitoring application that collects different cellular metrics of the BSs serving the user. The measurements were made outdoors and mainly by foot inside the TMC area with three LTE-A enabled smartphones, one for each operator. It is important to note that, due to municipal regulations, which impose a minimum distance of 100 m between a sensitive place and the BS, the TMC area does not have any BS installed in it, and thus, users are served by BSs outside TMC. These BSs were identified using the CellMapper application. Different zones of TMC experience very low values of the received power, which are equal or below −110 dBm. These results were manually confirmed by experiencing frequent drop calls and difficulty in accessing internet applications. The lack of installed BSs inside TMC has an impact on the quality of experience perceived by the user and on the type of service offered by the operator, and the regulation that integrates a minimum distance between the BS and a sensitive place has quite an impact on network planning.

III. Model Development and Simulator

A. Model Overview

The model configuration with its main inputs and outputs is represented in Figure 4.

The input parameters for the model are divided into environment, antenna, frequency bands, BS and usage. The environment parameters take the surroundings where the considered BS is inserted into account, which are classified as urban, suburban or rural. The antenna parameters, such as its dimension, input power, gain and frequency bands, are used as inputs for the exclusion zone evaluation, coverage and capacity models. The BS parameters, such as its height and type of installation, need to be considered as the propagation model inputs. The usage parameters take the type of service of the end-user into account, whether it is a voice service or a data one. The different types of services require different quality levels that influence the capacity of the cell as well as its radius.

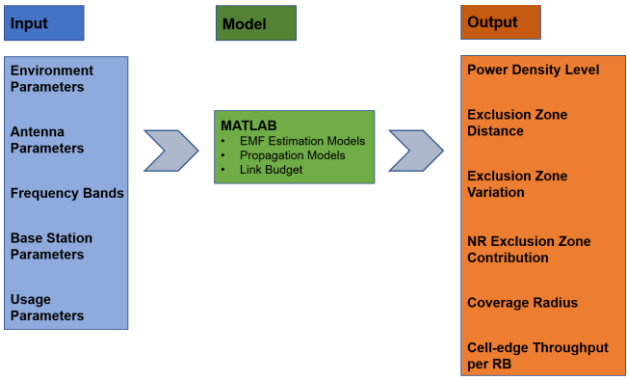

Figure 4. Model Configuration.

The output parameters are divided into power density level, exclusion zone distance, exclusion zone variation, NR exclusion zone contribution, coverage radius and throughput per RB at cell-edge. The developed model is able to compute the power density levels at any given instance from the antenna, enabling then the calculation of the exclusion zone distance and consequently the exclusion zone variation with the installation of the NR antenna. The coverage radius and throughput per RB are computed through the link budget equations present in this thesis and based on the works of [7] and [8]. The propagation models used are the Okumura-Hata for the NR 700 MHz band [9], and the WINNER II for the NR 3.6 GHz band [10].

Two situations are considered regarding exclusion zone evaluation via simulation: one considers only the legacy antenna and the other takes both the legacy and the NR antennas working simultaneously. The analysis of both simulations allows one to evaluate the power density levels before and after the installation of NR, allowing for the computation of the variation of the BS exclusion zone and also the contribution of NR to the obtained variation. Regarding the impact of the exclusion zone restrictions in the performance of NR BSs, reference values for the coverage radius and cell-edge throughput per RB are defined and then a comparison is made with the results obtained from the imposed restrictions. The simulations are performed in MATLAB.

In order to assess the developed models, a series of empirical tests were performed at the end of Chapter 3. Since the general model comprises two major parts, the exclusion zone evaluation, and the coverage and capacity planning, the assessment was divided accordingly. The tests and results are presented in this thesis.

B. Power Density Estimation Models

1) Far-Field Model

The far-field model is one of the most common EMF level estimation models and is also the simplest one. The RMS value for the power density being expressed by:

$$S(d,\theta,\varphi)_{[\mathrm{W/m^2}]} = \frac{P_{in\,[\mathrm{W}]}\ G(\theta,\varphi)}{4\pi\ d^2_{obs\,[\mathrm{m}]}}, d_{obs[\mathrm{m}]} \geq d_{ff\,[\mathrm{m}]} \quad (3.1)$$

$$d_{ff\,[\mathrm{m}]} = \frac{2\ D^2_{ant\,[\mathrm{m}]}}{\lambda_{[\mathrm{m}]}} \quad (3.2)$$

where:

- θ: elevation angle;
- φ: azimuth angle;
- P_{in}: input power of the antenna;

- $G(\theta, \varphi)$: antenna gain in the direction of the elevation and azimuth angles;
- d_{ff}: far-field distance;
- D_{ant}: the largest dimension of the antenna.

Although the far-field model is of great simplicity, its range of applicability is rather limited, as it can only be applied when the distance from the antenna to the observation point is greater than the far-field distance of the antenna under study. If the far-field model is applied in the near-field region of the antenna, the computed field strength is overestimated.

2) Far-Field Gain-Based Model

The far-field gain-based model is a fast and efficient method for the evaluation of EMF levels inside the near-field region of the BS antenna [5]. For this method, the gain of the entire antenna is derived from the combination of the far-field radiation pattern of an antenna element with the array factor. The model considers that BS antennas are uniform arrays and that the coupling between the dipoles of the array can be neglected. A good estimate of the near-field can thus be obtained as a combination of the far-field radiated by each antenna element:

$$S(d,\theta,\varphi)_{[\mathrm{W/m^2}]} \approx \frac{\left|\sum_{i=1}^{N_{el}} \frac{\sqrt{30\ P_{i,in\,[\mathrm{W}]}\ G_{el}(\theta_i,\varphi_i)}}{d_{i,obs\,[\mathrm{m}]}} e^{-j(k_0 d_{i,obs}+\psi_i)}\ \hat{r}(\theta_i,\varphi_i)\right|^2}{Z_{0[\Omega]}},$$

$$d_{obs\,[\mathrm{m}]} > 3\lambda_{[\mathrm{m}]} \tag{3.3}$$

$$G_{el}(\theta_i,\varphi_i) \approx \frac{G_M\ D_{V,el}(\theta_i)\ D_{H,el}(\varphi_i)}{N_{el}} \tag{3.4}$$

$$k_{0\,[\mathrm{rad/m}]} = \frac{2\pi}{\lambda_{[\mathrm{m}]}} \tag{3.5}$$

where:

- N_{el}: number of radiating elements of the antenna;
- $P_{i,in}$: input power to the the i^{th} element;
- θ_i: elevation angle of the i^{th} element relative to point of observation;
- φ_i: azimuth angle of the i^{th} element relative to point of observation;
- $d_{i,obs}$: distance from the i^{th} element to the point of observation;
- $\hat{r}(\theta_i,\varphi_i)$: unitary vector of the i^{th} element;
- $G_{el}(\theta_i,\varphi_i)$: antenna element gain;
- G_M: maximum antenna gain;
- $D_{V,el}(\theta)$: element radiation pattern in the vertical plane;
- $D_{H,el}(\varphi)$: element radiation pattern in the horizontal plane;
- ψ_i: phase shift of the i^{th} element.
- k_0: free space wavenumber.

Note that in (3.3) the expression inside the absolute value bars corresponds to the radiated electric field.

C. Exclusion Zone Evaluation Model

1) Far-Field Zone

For the purpose of this thesis, the only sources of radiation are the BS antennas since the exposure from other sources inside the exclusion zone is rather weak in comparison, thus, only the frequencies used in the BS are considered and the exposure from other sources is assumed to be zero. Taking this into consideration, (2.1) can be rewritten as:

$$S_{norm}^{tot} = \sum_{i=1}^{N_{sys}} \left(\frac{S_{i\,[\mathrm{W/m^2}]}}{S_{ref,i\,[\mathrm{W/m^2}]}} \right) \leq 1 \tag{3.6}$$

where:

- N_{sys}: the number of communications systems used in the BS;
- S_{norm}^{tot}: the total normalised power density.

Taking (3.6) as a reference, the goal is to calculate a distance such that the total normalised power density is equal to 1. This distance, in the direction of maximum radiation, is the value for the front border of the exclusion zone, D_{front}.

In order to compute the power density in the far-field region of an antenna, (3.1) is used. Combining (3.1) with (3.6) one has:

$$S_{norm}^{tot} = \sum_{i=1}^{N_{sys}} \left(\frac{P_{i\,[\mathrm{W}]}\ G_{M,i}}{4\pi\ d_{obs\,[\mathrm{m}]}^2}\ \frac{1}{S_{ref,i\,[\mathrm{W/m^2}]}} \right) \tag{3.7}$$

where:

- P_i: the input power for the i^{th} system;
- $G_{M,i}$: the maximum antenna gain for the i^{th} system.

The front border of the exclusion zone is such that S_{norm}^{tot} must be equal to 1 at that distance. Taking into account this and the fact that the d_{obs} is the same for all used frequencies, D_{front} can be computed as follows:

$$\frac{1}{D_{front\,[\mathrm{m}]}^2} \sum_{i=1}^{N_{sys}} \left(\frac{P_{i\,[\mathrm{W}]}\ G_{M,i}}{4\pi}\ \frac{1}{S_{ref,i\,[\mathrm{W/m^2}]}} \right) = 1 \tag{3.8}$$

and so:

$$D_{front\,[\mathrm{m}]} = \sqrt{\sum_{i=1}^{N_{sys}} \left(\frac{P_{i\,[\mathrm{W}]}\ G_{M,i}}{4\pi}\ \frac{1}{S_{ref,i\,[\mathrm{W/m^2}]}} \right)} \tag{3.9}$$

One should notice that if the computed D_{front} is less than the minimum distance that contains all the BS's far-field distances, then the exclusion zone is inside the near-field of the BS and thus a near-field model is needed to compute the EMF exposure.

2) Near-Field Zone for Linear Arrays

In order to use the far-field gain-based model for the computation of the EMF exposure in the near-field of the antenna, first one needs to define the geometry of the problem. Figure 5 represents the considered geometries for both even and odd numbers of elements in a uniform array.

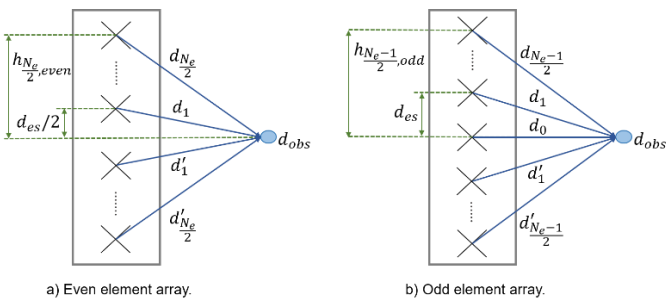

a) Even element array. b) Odd element array.

Figure 5. Geometry comparison between even and odd element arrays.

The point of observation is at a distance d_{obs} from the antenna and it is chosen to have a height that corresponds to the midpoint of the antenna. Due to the existing symmetry, one can now make the analysis of the problem focusing only on half of the array elements.

The distance from the i^{th} element of the array to the point of observation $d_{i,obs}$ can be described as a function of d_{obs}. This work considers only even element arrays and thus, expressions for odd element arrays are not presented although they are similarly derived. According to Figure 5, for an array with an even number of elements, the expression for $d_{i,obs}$ as a function of d_{obs} is given by:

$$d_{i,obs\,[\mathrm{m}]} = \sqrt{h_{i,even\,[\mathrm{m}]}^2 + d_{obs\,[\mathrm{m}]}^2} \tag{3.10}$$

$$h_{i,even\,[\mathrm{m}]} = \frac{(2i-1)}{2}\ d_{es\,[\mathrm{m}]} \tag{3.11}$$

where:

- $h_{i,even}$: the distance from the i^{th} element centre to the array centre for an even element array;
- d_{es}: the distance between each element.

From the considerations adopted above, the electric field expression from (3.3) can be rewritten as:

$$E(d,\theta,\varphi) \approx \left| \sum_{i=1}^{\frac{N_{el}}{2}} \frac{2\sqrt{30\ P_{i,in}\ G_{el}(\theta_i,\varphi_i)}}{d_{i,obs}} e^{-j(k_0 d_{i,obs}+\psi_i)} \right| \tag{3.12}$$

The direction of maximum radiation is considered to be perpendicular to the antenna axis ($\theta = \pi/2$) and thus $\psi_i = 0$. It is also assumed that the array power efficiency is equal to 1 and that the input power is equally distributed over all elements.

The gain of one element is given by (3.4) and it depends on N_{el}, G_M, the element vertical radiation pattern, $D_{V,el}(\theta)$, and the element horizontal radiation pattern, $D_{H,el}(\varphi)$. The horizontal radiation pattern for a dipole is omnidirectional and therefore it is considered to be equal to 1. The vertical radiation pattern is a well-known function of the elevation angle and the dipole's length relative to the wavelength, being defined as [11]:

$$D_{V,el}(\theta) = \left| \frac{\cos\left(\frac{k_0 L_{dip\,[\mathrm{m}]}}{2}\cos(\theta)\right) - \cos\left(\frac{k_0 L_{dip\,[\mathrm{m}]}}{2}\right)}{\sin(\theta)} \right|^2 = |F_P(\theta)|^2 \tag{3.13}$$

where:

- L_{dip}: the dipole's length;
- $F_P(\theta)$: the radiation pattern factor.

Since the model analysis takes advantage of the symmetry between the upper and lower half of the array, it is easier to analyse the contribution of each element if θ is replaced by the angle formed by the element's horizontal axis and the direction of observation (θ'):

$$\theta' = \frac{\pi}{2} - \theta \tag{3.14}$$

Taking all the previous considerations into account, the gain of each element, given by (3.4), can be rewritten as:

$$G_{el}(\theta_i') \approx \frac{G_M}{N_{el}}\ |F_P(\theta_i')|^2 \tag{3.15}$$

where:

$$F_P(\theta_i') = \frac{\cos\left(\frac{k_0 L_{dip}}{2}\cos\left(\frac{\pi}{2}-\theta_i'\right)\right) - \cos\left(\frac{k_0 L_{dip}}{2}\right)}{\sin\left(\frac{\pi}{2}-\theta_i'\right)} \tag{3.16}$$

All the relevant elements for the far-field gain-based model are now fully defined and thus (3.12) can be further simplified:

$$E(d,\theta_i') \approx \frac{2\sqrt{30P_{in}G_M}}{N_{el}} \left| \sum_{i=1}^{\frac{N_{el}}{2}} \frac{|F_P(\theta_i')|}{d_{i,obs}} e^{-jk_0 d_{i,obs}} \right| \tag{3.17}$$

3) Near-Field Zone for Planar Arrays

In order to assess exposure from a planar array, a different geometrical approach is taken. Figure 6 represents the coordinate system for a planar array, where both antenna elements and observation point are represented in a 3D space, the antenna being placed at the zOy plane ($x = 0$).

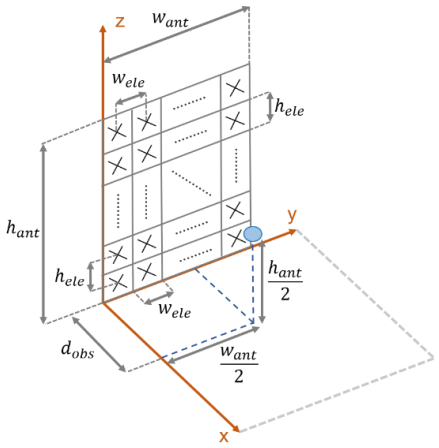

Figure 6. Coordinates system for a planar array antenna.

The observation point is assumed to be at a distance d_{obs} from the antenna centre. To simplify the analysis, one assumes that each element occupies a rectangle with width w_{ele} and height h_{ele} given by:

$$h_{ele\,[\mathrm{m}]} = \frac{h_{ant\,[\mathrm{m}]}}{N_{V,el}} \tag{3.18}$$

$$w_{ele\,[\mathrm{m}]} = \frac{w_{ant\,[\mathrm{m}]}}{N_{H,el}} \tag{3.19}$$

where:

- h_{ant}: the height of the antenna;
- w_{ant}: the width of the antenna;
- $N_{V,el}$: the number of vertical elements of the planar array;
- $N_{H,el}$: the number of horizontal elements of the planar array.

Assuming that each element is placed at the centre of each rectangle, the y and z coordinates of the element placed in the i^{th} line and j^{th} column are expressed respectively by:

$$y_{ij\,[\mathrm{m}]} = \frac{w_{ele\,[\mathrm{m}]}}{2} + (j-1)\ w_{ele\,[\mathrm{m}]} \tag{3.20}$$

$$z_{ij\,[\mathrm{m}]} = \frac{h_{ele\,[\mathrm{m}]}}{2} + (i-1)\ h_{ele\,[\mathrm{m}]} \tag{3.21}$$

Taking the previous considerations into account, the distance from an element to the observation point is expressed as follows:

$$d_{ij,obs} = \sqrt{{d_{obs}}^2 + \left(y_{obs} - y_{ij}\right)^2 + \left(z_{obs} - z_{ij}\right)^2} \tag{3.22}$$

where:

- y_{obs}: the y coordinate of the observation point $(w_{ant}/2)$;
- z_{obs}: the z coordinate of the observation point $(h_{ant}/2)$.

It is assumed that the total power is equally distributed over all elements:

$$P_{el\,[\mathrm{W}]} = \frac{P_{in\,[\mathrm{W}]}}{N_{el}} = \frac{P_{in\,[\mathrm{W}]}}{N_{V,el}\ N_{H,el}} \tag{3.23}$$

Taking all the previous considerations into account, the electric field for a planar array in the near-field is given by:

$$E(d,\theta_{ij}) \approx \frac{\sqrt{30\ P_{in}\ G_M}}{N_{el}} \left| \sum_{i=1}^{N_{V,el}} \sum_{j=1}^{N_{H,el}} \frac{|F_P(\theta_{ij})|}{d_{ij,obs}} e^{-jk_0 d_{ij,obs}} \right| \tag{3.24}$$

where:

- θ_{ij}: elevation angle of an element in relation to the observation point.

4) General Zone Model

In order to account for the monotonically decreasing behaviour of the power density with distance, an interpolation method is applied in the near-field. The interpolation function that best suits the power density behaviour depends on the number of vertical elements, or simply the number of elements for linear arrays, being:

$$S_{fit}(d) = \begin{cases} \frac{P_{in}G_M}{4\pi} \frac{1}{(a_0 + a_1 d + a_2 d^2)}, & N_{el}, N_{V,el} < 8 \\ \frac{P_{in}G_M}{4\pi} \frac{1}{(a_0 + a_1 d + a_2 d^2 + a_3 d^3)}, & N_{el}, N_{V,el} \geq 8 \end{cases} \tag{3.25}$$

where a_0, a_1, a_2 and a_3 are the coefficients of the rational function $S_{fit}(d)$. One should note that these coefficients are normalised to the input power and gain of the antenna. The interpolation is based on the maxima of $S(d)$ and, since $S(d)$ may have a low number of maxima, equally spaced points along the power density curve after the last maximum are also used.

The obtained function $S_{fit}(d)$ may have, for a given distance, lower values than $S(d)$. To ensure the worst-case scenario, the upper bound method is used [2], i.e., the largest relative difference between $S_{fit}(d)$ and $S(d)$ is applied to $S_{fit}(d)$, ensuring then that $S_{fit}(d)$ is vertically moved.

For distances above the far-field one, the far-field model becomes more accurate and, due to its simplicity, it is used in such circumstances. In order for the complete model to be realistic, it needs to vary continuously from the near-field zone to the far-field one since EMFs vary continuously as a function of distance. This continuity can be ensured by applying a final interpolation with the final point being at the far-field distance with the far-field value for the power density. The interpolation function is also given by (3.25). The final power density expression is then as follows:

$$S_{final}(d) = \begin{cases} S_{near-field}(d), & 3\lambda \leq d < d_{ff} \\ \frac{P_{in}G_M}{4\pi d^2}, & d \geq d_{ff} \end{cases} \tag{3.26}$$

where:

- $S_{near-field}(d)$: the final interpolation function obtained for the power density in the near-field.

Under the circumstances of the developed model, the total normalised power density as a function of distance is given by:

$$S_{norm}^{tot}(d) = \sum_{i=1}^{N_{sys}} \left(\frac{S_{final,i}(d)}{S_{ref,i}} \right) \tag{3.27}$$

where:

- $S_{final,i}(d)$: power density function obtained by the model for the i^{th} communication system.

As previously mentioned, the distance D_{front} is such that the total normalised power density is equal to 1. Since solving (3.27) as a function of distance has great computation complexity, considering that $S_{norm}^{tot}(d)$ is a function of N_{sys} terms with 2 equations to describe each one, instead (3.27) is iterated over the distance samples. D_{front} is then given by the minimum distance that ensures $S_{norm}^{tot}(d) < 1$.

In order to compute the complete BS exclusion zone, the distances for the remaining directions are calculated by either applying correction factors to D_{front} or to the antenna gain. From the analysis of the radiation patterns of each system, the normalised gains for each direction are extracted and applied as correction factors for the antenna gain.

D. Comparison with Experimental Results

Experimental EMF measurements were conducted in operational BSs in order to analyse the real behaviour of the power density in the vicinity of the BSs' antennas. These measurements allow for the comparison of the measured data with the developed theoretical model, thus evaluating its deviation from the experimental results.

In order to evaluate the performance of the theoretical model against the experimental data, the total average difference between the model's results and the measurements, μ_{model}, and its corresponding standard deviation, σ_{model}, were analysed. The results are presented in Table 3. Note that measurements were performed for the back of the antennas (180º), front (0º), and diagonally (45º and 315º).

Table 3. Results for the performance of the theoretical model compared to measurements.

System	μ_{model} [dB]		σ_{model} [dB]
	0º/45º/315º	180º	
GSM900	7.25	14.00	3.48
UMTS2100	9.41	18.36	4.32
LTE1800	14.06	17.12	4.34
NR3600	38.17		6.02

The results from the performance evaluation suggest that the model's results correctly follow the measurements' behaviour, due to the relatively low values of σ_{model}, and that it overestimates exposure levels. The proposed model is then a practical tool for the estimation of power density levels in the vicinity of the BS, and consequently exclusion zone distances, with a confident safe margin as indicated by the performance results.

IV. Results Analysis

A. Scenarios Description

The variation of the EMF levels on BSs before and after the installation of NR, as well as the BS performance regarding coverage radius and throughput per RB, were evaluated by applying the developed models to representative cases of BS installations possessing GSM, UMTS and LTE. The scenarios chosen for this purpose are presented in Table 4, as well as the corresponding systems.

The output powers per carrier/MIMO element for each system present in the considered scenarios are represented in Table 5. Note that multiple carriers are transmitted only in GSM and UMTS, while MIMO is only implemented in LTE and NR. The number of MIMO elements for each LTE and NR band is presented in Table 6.

Table 4. Used mobile communications systems in each scenario.

Scenarios	Mobile Communications Systems Frequency Bands								
	GSM	UMTS		LTE				NR	
	900	900	2100	800	1800	2100	2600	700	3600
Urban.1	X		X		X				X
Urban.2	X		X				X		X
Urban.3	X		X		X		X		X
Suburban.1	X	X	X	X	X				X
Suburban.2	X	X		X		X		X	
Suburban.3	X		X	X	X	X		X	X
Rural.1	X	X		X				X	
Rural.2	X	X	X			X		X	
Rural.3	X	X	X	X		X		X	

Table 5. Output power per carrier/MIMO element and antenna gain for the systems under analysis.

System			Output Power per Carrier/MIMO Element [W]	Maximum Antenna Gain [dBi]
GSM	900		20	16.0
UMTS	900		20	16.0
	2100		30	15.9
LTE	800		40	15.5
	1800			15.5
	2100		10	15.9
	2600		40	16.7
NR	700		40	15.2
	3600	AAU5613	2.5	25.0
		AAU5339w	5	23.8

The exclusion zone distances for the direction of maximum radiation, D_{front}, were computed for different number of carriers for GSM ($N_{c\ GSM900}$) and UMTS ($N_{c\ UMTS}$), since for any BS installation, the number of carriers used in a system may differ. Four different configurations on the ratio $N_{c\ GSM900}/N_{c\ UMTS}$ were used to obtain a wide variety of results: 1/1, 2/1, 4/2 and 4/4; $N_{c\ UMTS}$ refers to the number of carriers for both the 900 and 2100 bands.

The analysis for this thesis was performed using two different active antennas for the NR3600 band. For the urban scenarios one considered the AAU5613 antenna and for the suburban scenarios the AAU5339w one (these are antennas manufactured by Huawei).

Table 6. Number of MIMO elements for each band of LTE and NR.

System			Number of MIMO Elements
LTE	800		2
	1800		
	2100		
	2600		4
NR	700		2
	3600	AAU5613	64
		AAU5339w	32

The values used for the link budget parameters are presented in Table 7, which are reference values, extracted from [12], for the DL channel, since it is the connection of interest for this thesis. Since the scope of this thesis is to analyse the impact of EMF restrictions solely on outdoors BSs, indoors users served by indoors BSs are not considered.

Table 7. Reference values for the link budget parameters.

Parameter	Urban	Suburban		Rural
		NR3600	NR700	
Slow-Fading Margin [dB]	7.0	6.0		5.0
Interference Margin [dB]	6.0	4.0		2.0
Cable Losses [dB]	0.0	0.0	2.0	2.0
SCS [kHz]	30.0	30.0	15.0	15.0
Number of RBs	273	273	55	55
MT Height [m]	1.8			
BS Height [m]	42.0			
MT Antenna Gain [dBi]	3.0			
MT Losses [dB]	3.0			
MT Noise Figure [dB]	7.0			
SINR [dB]	5.0			
Coverage Probability [%]	90.0			
MIMO Order	2x2			

B. *Variation of D_{front}*

The computations of the exclusion zone distances were performed for the scenarios presented above using (3.26) for the power density contribution of each system and (3.27) to compute the exclusion zone distance.

The results of D_{front} for the carrier configurations 1/1 and 4/4 are presented respectively in Figures 7 and 8, considering the absence (W/O NR) and presence (W NR) of NR.

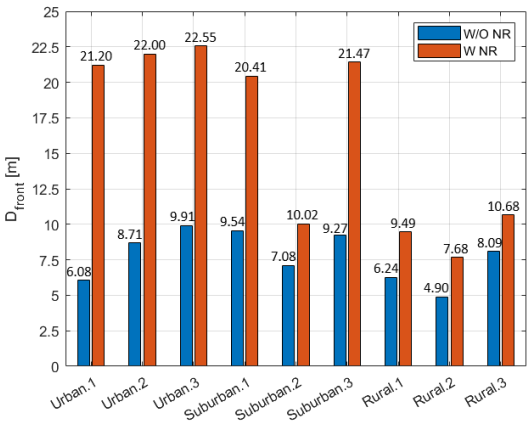

Figure 7. D_{front} results for the carrier configuration 1/1.

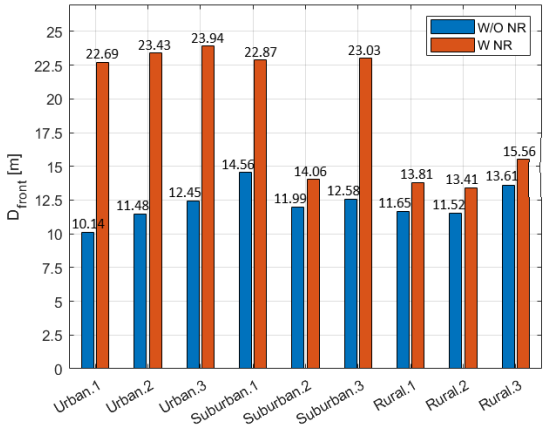

Figure 8. D_{front} results for the carrier configuration 4/4.

The increase in the compliance distance, for all configurations, due to the installation of NR ranges from 92.3% to 248.7% for the urban scenarios, from 17.3% to 131.6% for the suburban ones, and from 14.3% to 56.4% for the rural ones. One should note that the increase in D_{front} is overall lower for the rural scenarios since they only consider the deployment of NR700, as opposed to urban and suburban ones where NR3600 is installed.

Due to the high results for D_{front} in urban scenarios, between 21.20 m (Urban.1 with 1/1 configuration) and 23.94 m (Urban.3 with 4/4 configuration), there are some considerations to be taken into account regarding public exposure. For scenarios with the antennas installed close to the ground, Ufaçade and Upole installations, physical barriers may need to be implemented at street level due to the typical minimum height of 3 m. The use of high values for the downtilt also increases the amount of exposure at the street, Figure 9.

With the introduction of horizontal and vertical sweeping in NR active antennas, the range of directions that coincide with the maximum antenna gain is increased. The vertical sweeping increases then the exposure at street level by increasing the total inclination angle, ϕ_{total}.

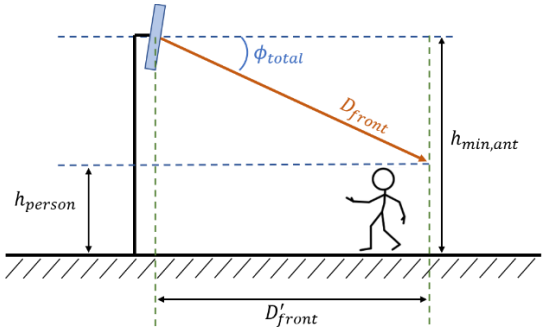

Figure 9. Downtilt and vertical sweeping influence on the exclusion region (adapted from [2]).

An evaluation can then be made to compute the minimum antenna height, $h_{min,ant}$, required in order not to install physical barriers. If the height of the antenna is above $h_{min,ant}$ no physical barriers are necessary, but, on the other hand, if the height of the antenna is below $h_{min,ant}$, D'_{front} corresponds to the distance at which physical barriers must be installed. The results were computed for the 4/2 and 4/4 carrier configurations, a downtilt of 12º, vertical sweeping of 30º, and h_{person} equal to 1.80 m.

According to the results, there is no need for physical barriers at ground level for urban BSs with a height higher than 12.67 m (Urban.3, 4/4 configuration, W NR). As observed in Table 2, the BS installations that may cause overexposure at street level are the Upole and Ufaçade topologies due to the low typical installation height. For Uroof scenarios, there may also be overexposure for BSs installed on top of small buildings in which the total antenna height is below 12 m above ground. For example, considering a building with 3 floors and 3 m per floor, [10], and an antenna installation height of 2 m, the total antenna height will be 11 m.

Another aspect to be taken into account is the impact of D_{front} on the buildings in front of the BS in Uroof scenarios. In these buildings, the rooftop, top floor balconies and/or top floor indoor spaces may be inside the BS's exclusion zone, depending on the width of the street. One assumes a sidewalk with a width of 2.25 m and each traffic lane with 3.5 m, [13], although these values may vary from place to place. For a street with 2 traffic lanes, the width of the street is 11.5 m, which is well below the 21.20 m obtained for D_{front} for Urban.1 with the 1/1 configuration. The top floor and rooftop of the frontal building would then be inside the BS's exclusion zone, assuming identical heights for the buildings.

C. *Exclusion Zone Variation for Other Directions*

In Table 8 is presented the analysed directions correspondent to D_{back}, D_{side}, D_{top}, and D_{bottom}. In Tables 9 and 10 are presented the results for Suburban.3 and Rural.3 respectively. A colour code scheme is presented in these results in order to better analyse the impact of NR on the exclusion zone distance in the direction of maximum radiation. For values of D_{front} up to 11.5 m, the results are considered acceptable and thus the colour is green. For $11.5 < D_{front\,[m]} \leq 15.0$, the results may be acceptable in some situations and thus the colour is orange, and for $D_{front\,[m]} > 15.0$ the colour is red. The values of 11.5 m and 15.0 m correspond to the width of a street with 2 and 3 traffic lanes respectively, as assumed in the previous section.

Table 8. Analysed directions for the back, side, top and bottom borders of the exclusion zone.

Back (H plane)	Side (H plane)	Top (V plane)	Bottom (V plane)
180º	90º and 270º	270º	90º

Table 9. Exclusion borders for the front, back, side, top and bottom for the Suburban.3 scenario.

	$N_{c\,GSM900}/N_{c\,UMTS}$		D_{front} [m]	D_{back} [m]	D_{side} [m]	D_{top} [m]	D_{bottom} [m]
Suburban.3	1/1	W/O NR	9.27	1.10	1.10	1.10	1.10
		W NR	21.47	1.18	3.72	1.18	1.18
	2/1	W/O NR	9.95	1.10	1.10	1.10	1.10
		W NR	21.76	1.18	3.74	1.18	1.18
	4/2	W/O NR	11.68	1.10	1.10	1.10	1.10
		W NR	22.63	1.18	3.80	1.18	1.18
	4/4	W/O NR	12.58	1.10	1.10	1.10	1.10
		W NR	23.03	1.18	3.83	1.18	1.18

Table 10. Exclusion borders for the front, back, side, top and bottom for the Urban.3 scenario.

	$N_{c\,GSM900}/N_{c\,UMTS}$		D_{front} [m]	D_{back} [m]	D_{side} [m]	D_{top} [m]	D_{bottom} [m]
Urban.3	1/1	W/O NR	9.91	0.95	0.95	0.95	0.95
		W NR	22.55	1.09	4.25	0.95	0.95
	2/1	W/O NR	10.38	0.95	0.95	0.95	0.95
		W NR	22.83	1.09	4.27	0.95	0.95
	4/2	W/O NR	11.71	0.95	0.95	0.95	0.95
		W NR	23.56	1.10	4.33	0.95	0.95
	4/4	W/O NR	12.45	0.95	0.95	0.95	0.95
		W NR	23.94	1.11	4.35	0.95	0.95

Regarding the suburban and rural scenarios, for the installations W NR, the highest working wavelength corresponds to NR700, except in Suburban.1, where NR3600 is installed instead, and thus LTE800 has the highest wavelength. For the suburban scenarios, the distances for the back, top and bottom are less than $3\lambda_{LTE800}$ or $3\lambda_{NR700}$. Note that $3\lambda_{LTE800} = 1.10$ m and $3\lambda_{NR700} = 1.18$ m.

For the urban environments W/O NR, the exclusion zone border for the back, side, top and bottom of the antenna is less than $3\lambda_{GSM900}$, 0.95 m. After the installation of the active antenna, the distances for the top and bottom of the antenna remain less than $3\lambda_{GSM900}$. In these cases, the compliance distance is below the range of the model and thus the border is set at this value.

Regarding the suburban and rural environments, there is no need for physical barriers in any direction since, as observed in Table 2, the antennas are typically installed in towers 20 to 50 m high with no access to the general public.

Considering the urban scenarios analysed in this thesis, the values for D_{top} and D_{bottom} are reduced and may not present the need to install public protection barriers. Regarding D_{top}, its value is below 0.95 m and also the top of the antenna is not usually accessed by the general public, and thus a physical barrier is not necessary. Regarding D_{bottom}, the concern might be the users on the top floor of the building, for Uroof scenarios and, depending on the installation's location, the public access

to the bottom part of the antennas. For Utower scenarios, the general public is not allowed and thus physical barriers are not necessary. For the Uroof scenarios, depending on the type of access available to the general public and the height of the antennas, physical barriers might be required. Regarding the public on the top floor of the building, there is no cause for concern, since the attenuation caused by the roof (concrete and brick) is above 16 dB [12] and the height at which the antennas are installed, Table 2, provide additional safety.

For D_{back}, the values vary from 1.06 m (Urban.1 with 1/1 configuration) to a maximum of 1.11 m (Urban.3 with 4/4 configuration). As explained earlier, there is no need for physical barriers that comprise the back of the antennas for the Utower scenarios since these have no public access. For the Uroof scenarios, it should be considered whether the public has access to the zones comprising the back of the antenna. If the back of the antennas is easily accessible, then, according to the results, physical barriers need to be considered. Regarding the Ufaçade scenarios, there is usually no danger of exposure due to the attenuation of the outer wall of the building. This attenuation can range from 12 dB (12 cm plasterboard wall) to 58 dB (external wall plus 2 inner ones) [12].

For the sides of the antenna, the compliance distance increases significantly with the introduction of NR. This increase is due to the side gain of the active antennas being significantly higher than the side gain of the legacy systems. The values for D_{side} vary between 4.19 m (Urban.2 with 1/1 configuration) and 4.55 m (Urban.3 with 4/4 configuration). For the Ufaçade installation, the concern for high exposure levels may be the approximation of the antenna's laterals to zones with public access like windows and balconies. Regarding the Uroof installation, an evaluation should be made whether the public has access or not to the sides of the BS. If these zones are accessible, due to the considerable values for D_{side}, then protective barriers should be installed.

D. Influence on Coverage and Throughput

The scenarios to be analysed in this section are the urban and suburban ones with 4/2 and 4/4 carrier configurations. In order to analyse the impact of EMF restrictions on these scenarios, three maximum values were considered for D_{front}: 18.5 m, 15 m, and 11.5 m, which are the widths of streets with 4, 3, and 2 traffic lanes respectively. The aim is then to compute the reduction in the transmission power necessary to meet the requirements, for each scenario, and analyse the impact of such reduction on the coverage radius and cell-edge throughput per RB of NR BSs.

The results obtained for the NR transmitted power for carrier configurations 4/2 and 4/4 are presented in Tables 11 and 12, respectively. For both configurations, the transmitted powers were computed for all systems present in each scenario as shown in Table 4. For the 4/2 configuration, the transmitted powers were also computed in the absence of UMTS, and for the 4/4 configuration, the transmitted powers were computed without LTE800 for the suburban scenarios and 20% of LTE's maximum power for the urban ones.

Table 11. NR transmitted powers for carrier configuration 4/2.

Characteristics	D_{front} [m]	Transmitted Power [W]						
		Scenario						
		Urban.1	Urban.2	Urban.3	Suburban.1	Suburban.2	Suburban.3	
							NR3600	NR700
All Communications Systems	11.5	18	7	0	0	30	0	0
	15.0	52	45	35	29	-	27	40
	18.5	98	84	74	88	-	83	50
Without UMTS	11.5	25	14	5	10	78	5	10
	15.0	59	51	42	52	-	40	30
	18.5	105	91	81	112	-	90	59

Table 12. NR transmitted powers for carrier configuration 4/4

Characteristics	D_{front} [m]	Transmitted Power [W]						
		Scenario						
		Urban.1	Urban.2	Urban.3	Suburban.1	Suburban.2	Suburban.3	
							NR3600	NR700
All Communications Systems	11.5	11	0	0	0	0	0	0
	15.0	45	37	27	6	-	24	20
	18.5	90	76	67	65	-	76	40
Without LTE800 for Suburban and 20% of LTE for Urban	11.5	18	16	14	0	72	10	5
	15.0	52	51	49	32	-	44	40
	18.5	98	95	93	92	-	97	60

The reference values obtained for the coverage radius and throughput per RB at cell-edge for the urban and suburban scenarios are presented in Table 13, which were obtained for a transmitted power of 160 W for NR3600 and 80 W for NR700, and SINR equal to 5 dB.

The results for the reduction in coverage radius and throughput per RB are presented in Tables 14 to 17. A colour code scheme is also implemented in the results: a reduction in coverage radius and throughput up to 20% is considered acceptable and thus the assigned colour is green; for reductions up to 40%, the colour is orange; for a reduction higher than 40% the results are unacceptable and thus the colour is red. The "-" indicates that NR cannot be installed.

Table 13. Reference values obtained for the cell radius, and throughput per RB.

Environment		Transmitted Power [W]	Coverage Radius [km]	Throughput per RB [kbit/s]
Urban		160	0.35	333.1
Suburban	NR3600	160	0.49	333.1
	NR700	80	2.24	166.6

Table 14. Coverage radius variation for carrier configuration 4/2.

Characteristics	D_{front} [m]	$\Delta_{R_{cell}}$ [%]						
		Scenario						
		Urban.1	Urban.2	Urban.3	Suburban.1	Suburban.2	Suburban.3	
							NR3600	NR700
All Communications Systems	11.5	-45.7	-60.0	-	-	-25.0	-	-
	15.0	-28.6	-31.4	-34.3	-38.8	0.0	-40.8	-18.3
	18.5	-11.4	-17.1	-20.0	-16.3	0.0	-18.4	-12.9
Without UMTS	11.5	-40.0	-51.4	-62.9	-55.1	-0.9	-63.3	-45.5
	15.0	-25.7	-28.6	-31.4	-28.6	0.0	-32.7	-25.0
	18.5	-11.4	-14.3	-17.1	-10.2	0.0	-16.3	-8.5

Table 15. Coverage radius variation for carrier configuration 4/4.

Characteristics	D_{front} [m]	$\Delta_{R_{cell}}$ [%]						
		Scenario						
		Urban.1	Urban.2	Urban.3	Suburban.1	Suburban.2	Suburban.3	
							NR3600	NR700
All Communications Systems	11.5	-54.3	-	-	-	-	-	-
	15.0	-31.4	-34.3	-40.0	-61.2	0.0	-42.9	-33.5
	18.5	-14.3	-20.0	-22.9	-24.5	0.0	-20.4	-18.3
Without LTE800 for Suburban and 20% of LTE for Urban	11.5	-45.7	-48.6	-51.4	-	-3.1	-55.1	-55.4
	15.0	-28.6	-28.6	-28.6	-38.8	0.0	-32.7	-18.3
	18.5	-11.4	-14.3	-14.3	-16.3	0.0	-14.3	-8.0

Table 16. Throughput per RB variation for carrier configuration 4/2.

Characteristics	D_{front} [m]	$\Delta_{R_b^{RB}}$ [%]						
		Scenario						
		Urban.1	Urban.2	Urban.3	Suburban.1	Suburban.2	Suburban.3	
							NR3600	NR700
All Communications Systems	11.5	-48.7	-91.1	-	-	-4.1	-	-
	15.0	-5.9	-8.4	-15.0	-22.0	0.0	-25.3	-1.9
	18.5	-0.9	-1.6	-2.3	-1.4	0.0	-1.6	-0.9
Without UMTS	11.5	-29.3	-64.1	-95.9	-80.5	-0.1	-95.9	-42.1
	15.0	-4.3	-6.2	-9.9	-5.9	0.0	-11.0	-4.1
	18.5	-0.7	-1.2	-1.7	-0.6	0.0	-1.3	-0.5

Table 17. Throughput per RB variation for carrier configuration 4/4.

Characteristics	D_{front} [m]	$\Delta_{R_b^{RB}}$ [%] Scenario						
		Urban.1	Urban.2	Urban.3	Suburban.1	Suburban.2	Suburban.3 NR3600	Suburban.3 NR700
All Communications Systems	11.5	-76.6	-	-	-	-	-	-
	15.0	-8.4	-13.2	-25.4	-93.7	0.0	-31.3	-11.0
	18.5	-1.3	-2.1	-3.0	-3.3	0.0	-2.1	-1.9
Without LTE800 for Suburban and 20% of LTE for Urban	11.5	-48.7	-56.1	-64.1	-	-0.1	-80.5	-80.6
	15.0	-5.9	-6.2	-6.8	-18.0	0.0	-8.8	-1.9
	18.5	-0.9	-1.1	-1.1	-1.2	0.0	-1.0	-0.4

V. CONCLUSIONS

The goal of this thesis was to develop a model to estimate exclusion zones of BSs with co-location of NR with legacy systems, and in particular, to study the influence of the deployment of NR on the variation of the exclusion zones. As these zones are usually inside the near-field zone of the BS antennas, near-field models for linear and planar arrays were developed. A model was also developed in order to analyse how the influence of NR on the exclusion zones and the EMF restrictions in BSs impact the performance of the NR BSs in terms of coverage radius and cell-edge throughput.

The results from the measurement campaign show that, on average, the theoretical model overestimates the exposure levels and, due to the relatively low values of the standard deviation, it correctly follows the behaviour of the power density near the antenna, making it a practical tool for the estimation of power density levels in the vicinity of the BS.

The results for D_{front} clearly demonstrate the impact of NR, especially NR3600, on the variation of compliance distances. For the 1/1 configuration, D_{front} increases up to 10.68 m with NR700 and 22.55 m with NR3600, with variations between 32% and 248.7%. For the 2/1 configuration, the variation in D_{front} is between 27.8% and 213.4%, and for the 4/2 configuration D_{front} increases between 17.1% and 146.7%. Finally, for the 4/4 configuration, D_{front} increases from 14.3% to 123.8%, with values up to 15.56 m for NR700 and 23.94 m for NR3600.

Due to the relatively high values of D_{front} W NR urban scenarios, there may be overexposure at street level due to the reduced minimum height of Ufaçade and Upole installations, and thus physical barriers for public protection may be installed. For a downtilt of 12º and a vertical sweep of 30º, there is no need to install physical barriers at ground level if the BS is more than 12.67 m high.

Regarding the back, side, top, and bottom of the BS, the results obtained with NR are usually not a complication for rural and suburban environments due to the installation characteristics of the BSs and the relatively low values for the compliance distances. For the suburban scenarios, the maximum value for D_{side} is 3.83 m, and for the remaining directions the compliance distance is below 1.18 m ($3\lambda_{NR700}$). For the urban environments, the dimensions of D_{back} , D_{side} , D_{back} and D_{bottom} should be taken into account whenever the BS antennas may be accessible to the general public.

Regarding the coverage and throughput analysis, it is found that, in some situations, the size of the exclusion zone without NR does not allow its installation. For the cases where NR can be installed, the coverage radius decreases up to 62.9% for the urban scenarios and 63.3% for the suburban ones. Regarding the throughput per RB, whenever it is possible to deploy NR, the decrease can reach up to 95.9% for both urban and suburban scenarios.

From the results, it can be concluded that, due to the high values for the exclusion zone dimensions, operators may need to reduce the transmission power of NR antennas, or even increase the investment in order to install NR BSs without the presence of legacy systems. Operators may also need to re-evaluate exposure levels in the vicinity of BSs in order to verify if physical barriers for public protection need to be implemented. For BSs with co-location, the power transmitted by legacy systems may also need to be reduced in order to install NR, which can bring a lot of complexity in the deployment of NR networks. It can also be observed that for D_{front} equal to 15 and 18.5 m, the decrease in coverage radius is generally higher than the decrease in throughput. For these cases, it may be preferable to allow the reduction in throughput while maintaining the coverage radius. Also, for the highest values of D_{front} , the decommission or power reduction of legacy bands may not be necessary since the difference in throughput per RB is not significant and may not justify the compromise of legacy systems.

For future work, it would be interesting to study how the BS surrounding environment, such as the floor, building walls and antenna supports (such as masts and poles) influence the shape and size of exclusion zones. This could be accomplished with EM simulations using CST and Antenna Magus. Another interesting research would be to develop better techniques for measuring EMF exposure of MaMIMO systems near the BS in already loaded commercial NR networks, ensuring that exposure levels are as realistic as possible. These results could then be compared with new exposure assessment mathematical models for MaMIMO systems that consider factors such as BS utilisation and spatial distribution of users. One suggests also the study and development of near-field radiation pattern models as a function of distance, for linear and planar antenna arrays, in order to obtain more accurate results in near-field exposure estimation.

REFERENCES

[1] Statista - Number of mobile (cellular) subscriptions worldwide from 1993 to 2019, (https://www.statista.com/statistics/262950/global-mobile-subscriptions-since-1993), Dec. 2020.

[2] M.G.C. Antunes, *Estimation of exclusion regions in LTE base stations colocated with GSM/UMTS*, M.Sc. Thesis, Instituto Superior Técnico, University of Lisbon, Oct. 2012.

[3] ICNIRP, "ICNIRP Guidelines for Limiting Exposure to Electromagnetic Fields (100 kHz to 300 GHz)", *Health Physics Society*, Vol. 118, No. 5, 2020, pp. 483- 524.

[4] D. Sebastião, D. Ladeira, M. Antunes, C. Oliveira, L.M. Correia, "Estimation of Base Stations Exclusion Zones", *in Proc. of VTC'10 - 72nd IEEE Vehicular Technology Conference*, Ottawa, Canada, Oct. 2010.

[5] C. Oliveira, C. C. Fernandes, C. Reis, G. Carpinteiro, L. Ferreira, L.M. Correia, D. Sebastião, *Definition of Exclusion Zones around typical Installations of Base Station Antennas*, monIT Project, Report Int_Tec_0102_15_BSExclZones, Ver. 15, Instituto de Telecomunicações, Lisbon, Portugal, Feb. 2005.

[6] L. Chiaraviglio, A.S. Cacciapuoti, G. Martino, M. Fiore, M. Montesano, D. Trucchi, N.B. Melazzi, "Planning 5G Networks Under EMF Constraints: State of the Art and Vision", *IEEE Access*, Vol. 6, Sep. 2018, pp. 51021 - 51037.

[7] A.B. Vieira, *Analysis of 5G Cellular Radio Network Deployment over Several Scenarios*, M.Sc. Thesis, Instituto Superior Técnico, University of Lisbon, Nov. 2018.

[8] I. A. R. Belchior, *Evaluation of 5G Cellular Network Implementation over an Existing LTE One*, M.Sc. Thesis, Instituto Superior Técnico, University of Lisbon, Nov. 2018.

[9] L.M. Correia, *Mobile Communications Systems*, Lecture Notes, Instituto Superior Técnico, University of Lisbon, Portugal, 2020.

[10] WINNER II, *"WINNER II Channel Models - Part I Channel Models"*, V1.2, Feb. 2008.

[11] M.G. Silveirinha, *Antennas*, Lecture Notes, Instituto Superior Técnico, University of Lisbon, Portugal, 2020.

[12] Huawei, *5G Network Planning*, Presentation, 2019.

[13] IMTT, *Road Network - Planning and Design Principles* (in Portuguese), Instituto da Mobilidade e dos Transportes Terrestres, Mar. 2011 (http://www.imt-ip.pt/sites/IMTT/Portugues/Planeamento/DocumentosdeReferencia/PacotedaMobilidade/Paginas/QuadrodeReferenciaparaPlanosdeMobilidadeAcessibilidadeeTransportes.aspx).